ISSN 1063-7850, Technical Physics Letters, 2019, Vol. 45, No. 9, pp. 858–861. © Pleiades Publishing, Ltd., 2019.
Russian Text © The Author(s), 2019, published in Pis'ma v Zhurnal Tekhnicheskoi Fiziki, 2019, Vol. 45, No. 17, pp. 8–11.

Ink-Jet Printing of Polyaniline Layers for Perovskite Solar Cells

O. L. Gribkova[a]*, V. A. Kabanova[a], A. R. Tameev[a], and A. A. Nekrasov[a]

[a] *A.N. Frumkin Institute of Physical Chemistry and Electrochemistry, Russian Academy of Sciences, Moscow, 199071 Russia*

**e-mail: oxgribkova@gmail.com*

Received May 13, 2019; revised May 13, 2019; accepted May 16, 2019

Abstract—Polyaniline-based water-soluble ink has been developed to form hole-transport layers for perovskite solar cells by the ink-jet printing method. A study of the optical properties and surface morphology of layers composed of a complex of polyaniline and polysulfonic acid resulted in criteria determining the optimal conditions of their printing being suggested. The printed layers were found to be promising hole-transport layers for perovskite solar cells.

Keywords: perovskites, solar cells, polyaniline, atomic-force microscopy.

DOI: 10.1134/S1063785019090050

Recently, hybrid organo-inorganic solar cells (SCs) based on perovskites have been attracting close attention due to their advantages, such as the wide light absorption spectrum, comparatively simple method of layer deposition, and high efficiency [1] reaching a value of 23% [2].

Great attention is given both to developing the composition of a perovskite being used and to methods used to deposit its layer. An important role is also played by the selection of charge-transport layers in an SC and, in particular, by the development of new materials for hole-transport layers (HTLs). Such conducting polymers as poly(3,4-ethylenedioxythiophene) (PEDOT) and polyaniline (PANI) are promising materials for use as HTLs in perovskite SCs with an inverted structure. For example, the HTLs based on a water-soluble complex of poly(3,4-ethylenedioxythiophene) with polystyrene sulfonic acid (PEDOT–PSSA) are successfully used in the development of perovskite SCs [3]. The method of ink-jet printing of PEDOT–PSSA layers is one of promising and actively developed methods for fabrication of SCs [4].

The possibility of using PANI as the HTL in perovskite SCs was demonstrated in a number of studies [5–8], including the use of a water-soluble complex of PANI with PSSA [6] and a copolymer of PANI and PSSA [7]. However, an SC with a PANI-based HTL prepared by ink-jet printing has not been fabricated previously. The deposition of PANI layers by ink-jet printing has mostly been used to create biological and chemical sensors and supercapacitors [9–12]. In these cases, the printing ink was based on organic solvents.

At the same time, a chemical synthesis of PANI in the presence of poly-(2-acrylamido-2-methyl-1-propanesulfonic) acid (PAMPSA) makes it possible to obtain its stable aqueous dispersion (with the properties and composition of the dispersion being unchanged for more than 2 years) [13]. The possibility of using this complex in SCs with a photoactive layer based on the known composite of poly(3-hexylthiophene) (P3HT) and a fullerene derivative PC71BM was demonstrated in [14, 15]. PANI–PAMPSA layers were produced both by casting onto a horizontal substrate [14] and by the ink-jet printing method [15]. It was found that lowering the content of PAMPSA in the complex (to 1 : 1.25 and less) results in that a solid phase of PANI is formed in solution [13, 15], which rules out using the composition of 1 : 1.25 and less for ink-jet printing. In addition, raising the concentration of the monomer (to more than 0.01 M) and that of PAMPSA in a synthesis yields gel-like aggregates of the PANI–PAMPSA complex, which also fails to satisfy the requirements imposed on printing solutions. It has been shown using the example of an SC based on the photoactive composite P3HT : PC71BM that the best characteristics are exhibited by devices with a PANI–PAMPSA layer with an aniline : PAMPSA ratio of 1 : 1.5 mol/g-equiv of sulfo acid groups [15].

The goal of the present study was to determine the optimal mode of an ink-jet printing of an HTL from an aqueous solution of the PANI–PAMPSA complex in fabrication of a perovskite SC.

PANI was synthesized via oxidative polymerization of aniline at room temperature in the presence of PAMPSA ($MW \sim 2 \times 10^6$, Sigma-Aldrich) [13, 15].

The aqueous solution of the PANI–PAMPSA complex, developed for the printing, had a concentration of 3.4 mg/mL and dynamic viscosity of 1.8 cP. The solution viscosity was determined with an Ubbelohde viscometer at a temperature of 30°C [15]. The printing of PANI–PAMPSA onto a glass substrate with an optically transparent electrically conducting ITO (indium–tin oxide) layer heated to 28–30°C was performed with an Epson Stylus Photo P50 jet printer [15]. Number N of printed layers in the HTL was varied from 2 to 5.

The printed layers were transferred into the atmosphere of argon and annealed at 70°C for 10 min to remove residual water. A 400-nm-thick layer of the $CH_3NH_3PbI_3$ perovskite was deposited onto the PANI–PAMPSA layer by the method previously described in [16, 17]. Thereafter, the method of thermal evaporation in a vacuum was used to successively deposit the electron-transport layer of fullerene C_{60} (Ossila Ltd.), blocking layer of 2,9-dimethyl-4,7-diphenyl-1,10-phenanthroline (Sigma-Aldrich), and Al electrodes with thicknesses of 40, 7, and 80 nm, respectively.

The electronic absorption spectra of the PANI–PAMPSA and perovskite layers in the UV-vis and near-IR spectral ranges were recorded on a Shimadzu UV-3101PC double-beam spectrophotometer. Atomic-force microscopy (AFM) was performed by using an Enviroscope AFM-microscope with a Nanoscope V controller (Bruker). The layer thicknesses were determined with a KLA-Tencor D-100 Profiler stylus profile meter. The current–voltage characteristics of the SC samples were measured with a Keithley Source Measurement unit and Oriel 96000 solar simulator (Newport Corp.) at intensity P_{in} = 100 mW/cm^2 (AM1.5 conditions) in a glove-box with dry atmosphere of argon.

Figure 1 shows absorption spectra of layers of the PANI–PAMPSA complex for various numbers N. The spectra have the shape characteristic of the conducting form of PANI (emeraldine), peaked at a wavelength around 800 nm (Fig. 1, inset), which is associated with the absorption of localized polarons [18]. With increasing number of layers, the absorption of the PANI–PAMPSA film grows, but, on the whole, this contribution to the absorption of the perovskite layer (Fig. 1, curve *5*) is negligible. The absorption of the photoactive perovskite layer covers the whole visible spectral range.

Figure 2 presents AFM images of the surface a printed PANI–PAMPSA layer at $N = 4$. The layer is strongly nonuniform across its thickness. The image of its surface (Fig. 2a) shows dried drops with average diameter of 30 μm, and the depth from a dip to a drop edge is 40–60 nm. Within a drop (Fig. 2b), PANI–PAMPSA has a characteristic globular structure similar to that of a layer deposited by drop casting [14].

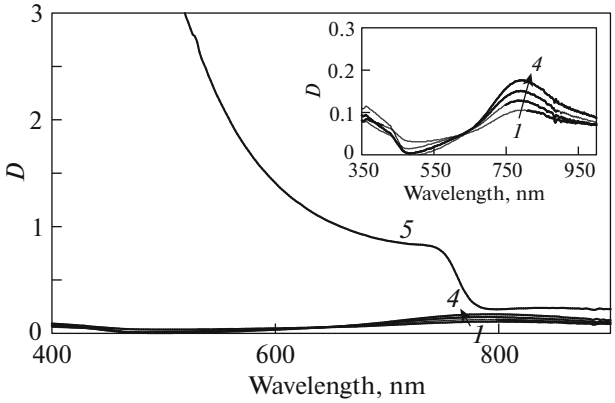

Fig. 1. Absorption spectra of a layer of the PANI–PAMPSA complex, produced by ink-jet printing at $N = 2$ (*1*), 3 (*2*), 4 (*3*), and5 (*4*), and of a perovskite layer deposited on a PANI–PAMPSA layer at $N = 4$ (*5*).

Microscale measurements of PANI layers with a profile meter demonstrated (Table 1) that the surface profile difference is at a maximum for $N = 2$. In this case, the layer has regions with thickness of less than 10 nm (up to its complete absence). With increasing N, the surface profile differences of the layers decrease owing to the more uniform distribution and overlapping of neighboring drops.

Figure 2c presents AFM images of the perovskite layer deposited above the PANI–PAMPSA layer. It can be seen that the average transverse diameter of crystals is 200–300 nm, with the maximum size reaching a value of 500 nm. It is known [1] that these sizes of microcrystals provide the highest efficiency of a perovskite SC. It is important to note that the surface morphology of the layers and the perovskite crystal sizes are independent of number N in the printing of a PANI layer.

Table 1 presents the photovoltaic characteristics of perovskite SCs with HTLs based on the PANI–PAMPSA complex. For each N, averaged values of the characteristics are presented measured on ten SCs. The spread of the values does not exceed 2% of the

Table 1. Characteristics of SCs with HTL based on the PANI–PAMPSA complex and produced by the ink-jet printing method

N	Δh, nm	J_{sc}, mA/cm^2	V_{oc}, V	FF	PCE, %
2	50 ± 5	17.08	0.85	0.64	9.25
3	40 ± 5	17.03	0.94	0.61	9.78
4	30 ± 5	18.37	0.94	0.61	10.57
5	20 ± 5	17.72	0.91	0.63	10.20

Note. Δh is the surface profile difference of a PANI–PAMPSA layer, J_{sc} is the short-circuit current, V_{oc} is the open-circuit voltage, FF is the fill factor, and PCE is the power conversion efficiency.

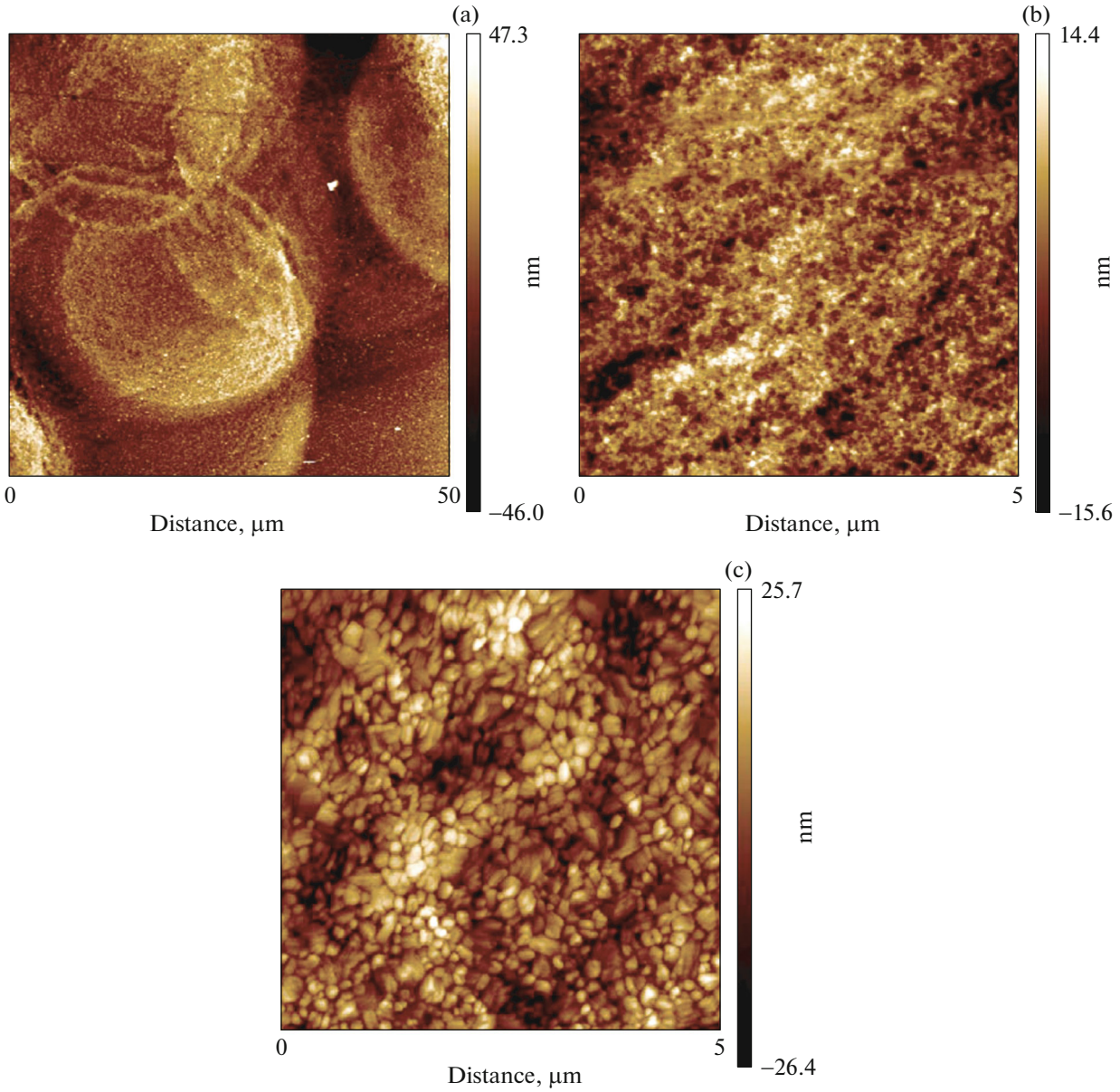

Fig. 2. AFM images of a PANI–PAMPSA layer produced by ink-jet printing at $N = 4$ on (a) 50- and (b) 5-μm scales and (c) that of the perovskite layer on a 5-μm scale.

average value. Analysis of the data in Table 1 shows that the surface profile differences decrease and the efficiency of the devices grows with increasing N. The maximum values of the efficiency and short-circuit current are observed for SCs with an HTL printed with $N = 4$, whereas, in the case of an HTL obtained at $N = 5$, the characteristics are poorer. We believe that, in samples with HTLs printed at $N = 2$ and 3, the ITO surface has areas uncovered by HTL, so the efficiency of hole transfer from perovskite to anode decreases and, as a consequence, the device efficiency drops. On the other hand, the smaller HTL profile difference at $N = 5$ makes the effective area of the interface between the HTL and the perovskite layer smaller as compared with HTL samples with $N = 4$.

Thus, the possibility of using the ink-jet printing method for deposition of an HTL based on the aqueous solution of the PANI–PAMPSA complex for a perovskite SC was demonstrated. The optimal number of printed PANI–PAMPSA layer in an HTL, at which the highest SC efficiency is provided, was found to be $N = 4$.

ACKNOWLEDGMENTS

Atomic-force microscopy and spectral measurements were performed at the Physical Methods of Investigation

Center for Collective Use of the Frumkin Institute of Physical Chemistry and Electrochemistry, Russian Academy of Sciences.

FUNDING

This study was financially supported by the Russian Science Foundation (project no. 18-13-00409) and by the Ministry of Science and Higher Education of the Russian Federation (in the part of research equipment).

CONFLICT OF INTEREST

The authors declare that they have no conflict of interest.

REFERENCES

1. H. S. Jung and N.-G. Park, Small **11**, 10 (2015).
2. N. J. Jeon, H. Na, E. H. Jung, T. Y. Yang, Y. G. Lee, G. Kim, H. W. Shin, S. I. Seok, J. Lee, and J. Seo, Nat. Energy **3**, 682 (2018).
3. S. Wang, T. Sakurai, W. Wen, and Y. Qi, Adv. Mater. Interfaces **5**, 1800260 (2018).
4. A. Singh, M. Katiyar, and A. Garg, RSC Adv. **5**, 78677 (2015).
5. K. Lee, H. Yu, J. W. Lee, J. Oh, S. Bae, S. K. Kim, and J. Jang, J. Mater. Chem. C **6**, 6250 (2018).
6. K. Lee, K. H. Cho, J. Ryu, J. Yun, H. Yu, J. Lee, W. Na, and J. Jang, Electrochim. Acta **224**, 600 (2017).
7. K.-G. Lim, S. Ahn, H. Kim, M.-R. Choi, D. H. Huh, and T.-W. Lee, Adv. Mater. Interfaces **3**, 1500678 (2016).
8. Y. Xiao, G. Han, Y. Chang, H. Zhou, M. Li, and Y. Li, J. Power Sources **267**, 1 (2014).
9. A. Chiolerio, S. Bocchini, and S. Porro, Adv. Funct. Mater. **24**, 3375 (2014).
10. M. V. Kulkarni, S. K. Apte, S. D. Naik, J. D. Ambekar, and B. B. Kale, Sens. Actuators, B **178**, 140 (2013).
11. K. Crowley, M. R. Smyth, A. J. Killard, and A. Morrín, Chem. Papers **67**, 771 (2013).
12. N. T. Brannelly and A. J. Killard, Talanta **167**, 296 (2017).
13. O. D. Iakobson, O. L. Gribkova, A. A. Nekrasov, V. A. Tverskoi, V. F. Ivanov, P. V. Mel'nikov, E. A. Polenov, and A. V. Vannikov, Prot. Met. Phys. Chem. Surf. **52**, 1005 (2016).
14. O. D. Iakobson, O. L. Gribkova, A. R. Tameev, A. A. Nekrasov, D. S. Saranin, and A. di Carlo, J. Ind. Eng. Chem. **65**, 309 (2018).
15. O. L. Gribkova, L. V. Saf'yanova, A. R. Tameev, D. A. Lypenko, V. A. Tverskoi, and A. A. Nekrasov, Tech. Phys. Lett. **44**, 239 (2018).
16. D. S. Saranin, V. N. Mazov, L. O. Luchnikov, D. A. Lypenko, P. A. Gostishev, D. S. Muratov, D. A. Podgorny, D. M. Migunov, S. I. Didenko, M. N. Orlova, D. V. Kuznetsov, A. R. Tameev, and A. di Carlo, J. Mater. Chem. C **6**, 6179 (2018).
17. O. D. Yakobson, O. L. Gribkova, A. R. Tameev, and E. I. Terukov, Tech. Phys. Lett. **45** (8), 794 (2019).
18. A. A. Nekrasov, V. F. Ivanov, and A. V. Vannikov, J. Electroanal. Chem. **482**, 11 (2000).

Translated by M. Tagirdzhanov